Effect of an Mg-Al insertion for directly sputtered MgAl$_2$O$_4$(001)-based epitaxial magnetic tunnel junctions

Mohamed Belmoubarik, Hiroaki Sukegawa, Seiji Mitani, and Kazuhiro Hono

National Institute for Materials Science
1-2-1 Sengen, Tsukuba 305-0047, Japan
Phone: +81-29-859-2000, E-mail: Belmoubarik.Mohamed@nims.go.jp

Abstract

We investigated the effect of an Mg-Al insertion on magneto-transport properties of epitaxial Fe/Mg$_{10}$Al$_{90}$ (Mg-Al) insertion/MgAl$_2$O$_4$ (1.9 nm)/Fe(001) magnetic tunnel junctions (MTJs). The tunnel magnetoresistance (TMR) ratio and differential conductance exhibited clear dependence on the inserted Mg-Al thickness. A slight Mg-Al insertion (thickness = 0.02–0.08 nm) was effective for obtaining a high TMR ratio and observing a local minimum structure in differential conductance curves, indicating the significant insertion effect on the MgAl$_2$O$_4$ barrier interface states. The present result shows the sensitivity of the interface states of MgAl$_2$O$_4$-based MTJs on the metallic layer insertion.

1. Introduction

Since TMR ratios over 100% at room temperature (RT) [1,2] were achieved in (001) MgO barrier-based MTJs, these devices attracted much interest because of their important role in the development of spintronics devices including magnetoresistive random access memories [3]. However, there could be a limitation of MgO-based MTJs performance because of the large lattice mismatch with various ferromagnetic materials. This suggests the importance of development a new type of barriers with tunable lattice constant while maintaining high TMR ratios.

The spinel MgAl$_2$O$_4$(001) barrier based MTJs prepared by Mg-Al post-oxidation have shown high TMR ratios over 100% at RT due to its very small lattice mismatch with bcc Co-Fe alloys (Fe(001) case, less than 0.3%) [4], and the occurrence of the spin-dependent coherent tunneling similar to the MgO(001) barriers as indicated by theoretical calculations [5,6]. Recently, a high quality and very flat *cation-disorder* MgAl$_2$O$_4$(001) barrier was developed by direct rf sputtering of an MgAl$_2$O$_4$ target, instead of the Mg-Al post-oxidation [7]. An Fe/MgAl$_2$O$_4$/Fe MTJ made by the direct sputtering showed a high TMR ratio up to 245% at RT. To obtain such a high TMR ratio, an insertion of an ultrathin Mg-Al metallic layer was effective. This suggests that the interface modification by a metallic insertion has a significant impact on the spin-dependent tunneling. Therefore, in this study, we investigated an effect of the Mg-Al insertion on TMR properties and differential conductance characteristics.

2. Experimental method

The MTJ multilayers were fabricated using a dc and rf magnetron sputtering system with a base pressure of 8 × 10^{-7} Pa and Ar gas. The MTJ stack consisted of an MgO(001) substrate/Cr (40)/Fe (100)/Mg$_{10}$Al$_{90}$ (Mg-Al) (t_{MgAl} = 0–0.6)/MgAl$_2$O$_4$ (1.9)/Fe (7)/Ir$_{20}$Mn$_{80}$ (12)/Ru (10) (unit in nm). Here, the Mg-Al layer was inserted using the wedge technique. The MgAl$_2$O$_4$ barrier was directly deposited from a stoichiometric MgAl$_2$O$_4$ sintered target. The deposition of each layer at RT was succeeded by an *in-situ* post-annealing at temperatures mentioned in Ref. [7]. Finally, the MTJ multilayers were annealed at 175°C under a magnetic field of 5 kOe. For the magneto-transport characterization, the MTJ stack was patterned into elliptical pillars with dimension of 5×10 μm^2 using photolithography and Ar ion-beam etching. The MTJs were characterized using a conventional dc 4-probe method at RT with the external magnetic field direction along Fe[100]. Here, a positive bias voltage indicates electron tunneling from the top electrode to the bottom one. More experimental details can be found in our previous report [7].

3. Results and discussion

The deposition optimization was performed by the post-annealing of sputtered layers simultaneously with an *in-situ* monitoring of film surface structures using reflection high-energy electron diffractions. These observations allowed the fabrication of high crystalline and lattice-matched Fe/MgAl$_2$O$_4$/Fe(001) MTJs, as reported in Ref. [7].

Figure 1 (a) shows examples of measured TMR ratio as a function of magnetic field for Mg-Al thickness t_{MgAl} = 0.02, 0.30 and 0.55 nm at RT. The highest TMR ratio of ~245% (resistance-area product of 5.24 kΩμm^2) was observed at t_{MgAl} = 0.02 nm. This high TMR ratio is sustained for t_{MgAl} up to 0.04 nm indicating the high quality of the bottom Fe/MgAl$_2$O$_4$ interface. Interestingly, t_{MgAl} = 0 showed a lower TMR ratio. The post-annealing process of an MgAl$_2$O$_4$ barrier deposited directly on an Fe electrode is thought to oxidize the Fe surface, and leads to a TMR ratio reduction.

t_{MgAl} dependence on the TMR ratio for Fe/Mg-Al(t_{MgAl})/MgAl$_2$O$_4$ (1.9 nm)/Fe MTJs is plotted in Fig. 1 (b). We observed three main TMR changes when t_{MgAl} increased. When t_{MgAl} is less than 0.08 nm, the TMR ratio is above 200% reflecting the high crystalline spinel MgAl$_2$O$_4$ barrier and lattice-matched Fe/MgAl$_2$O$_4$ interfaces. It should be mentioned that for the optimized MgAl$_2$O$_4$ deposition conditions on Fe electrode, we confirmed its *cation-disorder* nature [7]; which is the necessary condition to observe high TMR ratios (exceeding 200%) in Fe/MgAl$_2$O$_4$/Fe MTJs [4,5,7].
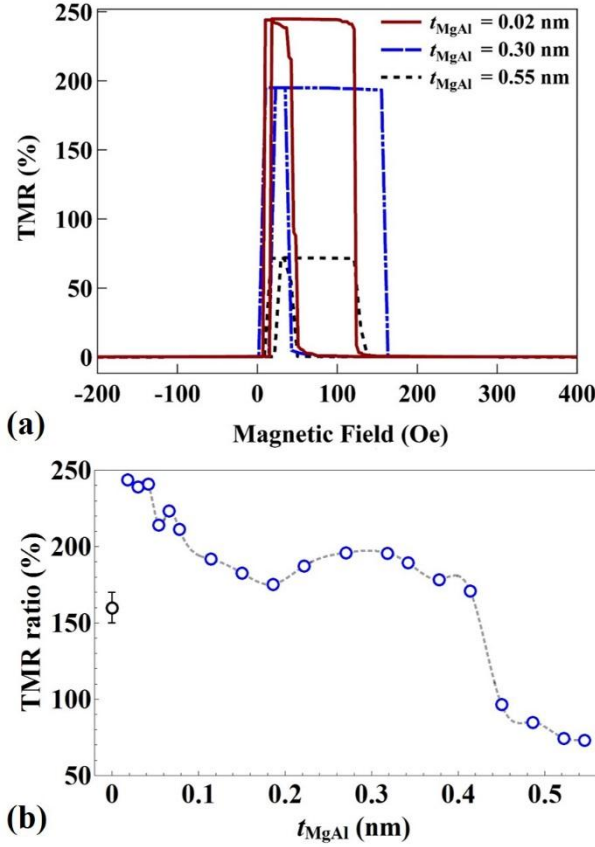
Fig. 1: (a) TMR ratios as a function of magnetic field of Fe/Mg-Al (t_{MgAl} = 0.02, 0.30 and 0.55 nm)/MgAl$_2$O$_4$ (1.9 nm)/Fe MTJs. (b) t_{MgAl} dependence of the TMR ratio for Fe/Mg-Al (t_{MgAl})/MgAl$_2$O$_4$ (1.9 nm)/Fe MTJs. These measurements were done at RT using 10 μA dc current (bias voltage ~several mV).

The second region of the TMR change is in the range of t_{MgAl} = 0.10–0.42 nm, which exhibited a TMR ratio between 170% and 200%. The third region where t_{MgAl} is above 0.44 nm, the TMR ratio dropped to less than 90%. This suggests a lowering of the barrier crystallinity and an increase of the inelastic scattering effect due to the presence of a non-oxidized Mg-Al region at the bottom-Fe/MgAl$_2$O$_4$ interface.

For an in-depth comparison of these three regions, we plotted the normalized differential conductance G_P (=dI/dV) for three representative devices in the magnetic parallel state: MTJ-A (TMR ~ 245%, t_{MgAl} = 0.02 nm), MTJ-B (TMR ~ 195%, t_{MgAl} = 0.30 nm), and MTJ-C (TMR ~ 73%, t_{MgAl} = 0.55 nm) as shown in Fig. 2. Local minima at around $|V|$ = 0.22 V were clearly observed for MTJ-A, implying the strong contribution of the coherent tunneling through the Fe electrodes and consistently with the obtained high TMR ratio [8]. For MTJ-B with a thicker Mg-Al insertion, the contribution of non-coherent tunneling may shift the local minima positions, and consequently reduced the TMR ratio. MTJ-C exhibited the most critical effect of the Mg-Al insertion by the vanishing of the local minima and the substantial reduction of the TMR ratio. The non-oxidized Mg-Al insertion at the bottom-Fe/MgAl$_2$O$_4$ interface and the oxygen deficient MgAl$_2$O$_4$ are thought to be responsible, as reported

in the MTJs fabricated by the post-oxidation of Mg-Al [8]. Therefore, the interface modification by the insertion layer is critical for achieving high TMR ratios in MgAl$_2$O$_4$-based MTJs.
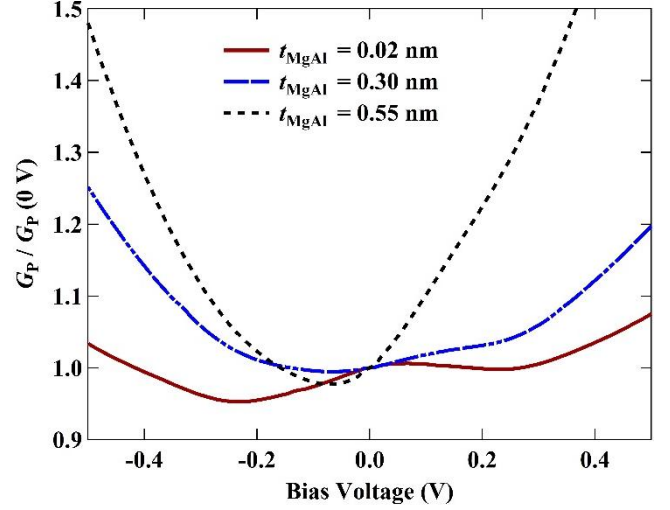
Fig. 2: G (=dI/dV) spectra of Fe/Mg-Al (t_{MgAl} = 0.02, 0.30 and 0.55 nm)/MgAl$_2$O$_4$ (1.9 nm)/Fe MTJs measured at RT at the parallel state.

4. Conclusions

The dependence of TMR ratio and differential conductance of (001)-oriented Fe/MgAl insertion/MgAl$_2$O$_4$/Fe MTJs on the Mg-Al thickness t_{MgAl} were investigated. The highest TMR ratio and a clear local minimum structure in the conductance curve were obtained for t_{MgAl} in the range of 0.02–0.08 nm. These results show the importance of the interface engineering for the improvement and control of MgAl$_2$O$_4$-based MTJs toward practical applications.

References
[1] S. S. P. Parkin, C. Kaiser, A. Panchula, P. M. Rice, B. Hughes, M. Samant, and S.-H. Yang, Nat. Mater. **3**, 862 (2004).
[2] S. Yuasa, T. Nagahama, A. Fukushima, Y. Suzuki, and K. Ando, Nat. Mater. **3**, 868 (2004).
[3] M. Gajek, J. J. Nowak, J. Z. Sun, P. L. Trouilloud, E. J. O'Sullivan, D. W. Abraham, M. C. Gaidis, G. Hu, S. Brown, Y. Zhu, R. P. Robertazzi, W. J. Gallagher, and D. C. Worledge, Appl. Phys. Lett. **100**, 132408 (2012).
[4] H. Sukegawa, Y. Miura, S. Muramoto, S. Mitani, T. Niizeki, T. Ohkubo, K. Abe, M. Shirai, K. Inomata, and K. Hono, Phys. Rev. B **86**, 184401 (2012).
[5] Y. Miura, S. Muramoto, K. Abe, and M. Shirai, Phys. Rev. B **86**, 024426 (2012).
[6] J. Zhang, X.-G. Zhang, and X. F. Han, Appl. Phys. Lett. **100**, 222401 (2012).
[7] M. Belmoubarik, H. Sukegawa, T. Ohkubo, S. Mitani, and K. Hono, Appl. Phys. Lett. **108**, 132404 (2016).
[8] H. Sukegawa, K. Inomata, and S. Mitani, Appl. Phys. Lett. **105**, 092403 (2014).